ICIC Express Letters
Volume **11**, Number **5**, May **2017**

 ISSN 1881-803X
pp. **967–976**

A NOVEL EXTEND-STATE-OBSERVER-BASED NONLINEAR OUTPUT FEEDBACK CONSTRAINED CONTROL FOR VARIABLE SPEED WIND TURBINES

Wenxu Yan[1], Xinmao Fang[1], Liang Geng[2], Lina Sheng[1], Gang Wang[1] and Dezhi Xu[1]

[1]Institute of Electrical Engineering and Intelligent Equipment
School of Internet of Things Engineering
Jiangnan University
No. 1800, Lihu Avenue, Wuxi 214122, P. R. China
lutxdz@126.com

[2]East South Asia, China Petroleum Pipeline Bureau
Langfang 062552, P. R. China

Received December 2016; accepted March 2017

Abstract. *In this paper, an extended state observer (ESO)-based nonlinear output feedback constrained control strategy is proposed for a variable speed wind turbine (VSWT). First, the dynamic model of VSWT is described. Next, a model transformation is proposed for VSWT dynamic model that converts the VSWT system into a strict-feedback form through state transformation. Then, an ESO is developed, which is used to design nonlinear output feedback constrained controller. In the design procedure of the controller, a novel dynamic anti-windup compensator is presented to deal with the magnitude and rate saturations of input. Finally, simulation results are given to demonstrate the effectiveness and potential of the proposed constrained control scheme.*
Keywords: Extended state observer, Control input saturation, Anti-windup, Variable speed wind turbine

1. **Introduction.** Wind is a kind of renewable energy with great potential. The wind power does not require the use of fuel and does not produce radiation or air pollution; it is forming a wave in the world [1-3].

Wind power is to turn the kinetic energy of the wind into the mechanical energy and convert the mechanical energy into the electricity kinetic energy. Wind capacity in the world has grown at a rate of 20%-30% per year over the past decade [4]. The wind turbine is an important component to turn the kinetic energy of the wind into the mechanical energy, which is composed of two (or more only) impellers in the shape of propeller. When the wind blows to the blade, the aerodynamic force generated on the blade drives the wind wheel rotation. Because the speed of the wind wheel is relatively low and the size and direction of the wind often change, leading to the unstable speed, before driving the generator, it is necessary to attach a transmission gear box to increase the rotation speed to the rated rotation speed of generator, and add a speed regulating mechanism for stable speed, and then connect to the generator.

With the development of control theory and technology of wind power generation, the wind power generator control system improves from the initial fixed pitch and constant speed control to the current variable pitch and variable speed control. Due to the great advantages of the variable speed wind turbines (VSWT) in the utilization of wind energy, the VSWT has become the main control study object [5-10]. Because of the factors of the inherent nonlinearity and uncertainty of wind turbine system and the existence of external operating condition effects, the controller designed by using the nominal linear

system model makes the robust performance of the actual system poor and reliability low. Therefore, in recent years, people have tried to use various nonlinear control theories based on models for studies on the control of wind turbine generator systems [7-11].

However, few modified control methods consider the actuator saturation problem. If the actuator saturation factor is not considered, the closed-loop control system may diverge. Many researchers have paid close attention to dynamical systems subject to input saturation due to the frequent occurrence in many systems. In linear systems, a general method to solve this problem of saturation is to treat the system as the sector nonlinearity [12,13]. The linear differential inclusion approach is another effective way for solving this problem; this strategy puts the saturated linear feedback inside the convex hull of the set in auxiliary linear feedbacks [14,15]. However, in nonlinear systems, there is no general effective method to deal with the saturation problem due to complex dynamic characteristics of the nonlinear systems. In [16], a new method of anti-windup compensator for nonlinear systems was proposed in the condition that people must find the equivalent functions to replace the original unknown nonlinear function. In practice, it is very difficult to realize.

In this paper, we give a novel nonlinear output feedback constrained control approach for VSWT. Inspired by the work of extended state observer (ESO) technique [17-19], we present a constrained control strategy after model transformation of VSWT via anti-windup approach. The major advantages of this dissertation are displayed as follows. In the design procedure of controller: 1) only the output measurement of VSWT is required; 2) explicit model dynamics and structural information of the VSWT do not need to be known; 3) the problem of input saturation in VSWT is considered and solved.

ω_r:	rotor speed (rad/s);	T_g:	generator electromagnetic torque (N· m);
ω_g:	generator speed (rad/s);	u_f:	field voltage (V);
υ:	wind speed (m/s);	L:	constant inductance of the circuit;
ρ:	air density (kg/m^3);	R_f:	resistance of the rotor field;
R:	rotor radius (m);	J_r:	rotor inertia (kg/m^2);
β:	pitch angle (rad);	K_r:	rotor external damping (H $\cdot$ m/rad $\cdot$ s);
T_a:	aerodynamic torque (N· m);	B_r:	rotor external stiffness (H $\cdot$ m/rad $\cdot$ s);
n_g:	gearbox ratio;	J_g:	generator inertia (kg/m^2);
T_{ls}:	low-speed torque (N· m);	K_g:	generator external damping (H $\cdot$ m/rad $\cdot$ s);
T_{hs}:	high-speed torque (N· m);	B_g:	generator external stiffness (H $\cdot$ m/rad $\cdot$ s);
I_f:	field current (A);	J_t:	turbine total inertia (kg/m^2);
K_ϕ:	machine-related constant;	B_t:	turbine total external stiffness (H·m/rad·s);
K_t:	turbine total external damping (H $\cdot$ m/rads);	T_{em}:	the generator torque (N· m).

2. **System Model and Problem Formulation.** The basic composition of VSWT includes three parts; they are wind turbines, growth container and generator. The block diagram of the variable speed wind turbine is shown in Figure 1.

The rotor dynamic is described as

$$J_r\dot{\omega}_r = T_a - K_r\omega_r - B_r\int_0^t \omega_r(\tau)\mathrm{d}\tau - T_{ls} \tag{1}$$

And the generator dynamic is given as

$$J_g\dot{\omega}_g = T_{hs} - K_g\omega_g - B_g\int_0^t \omega_g(\tau)\mathrm{d}\tau - T_g \tag{2}$$

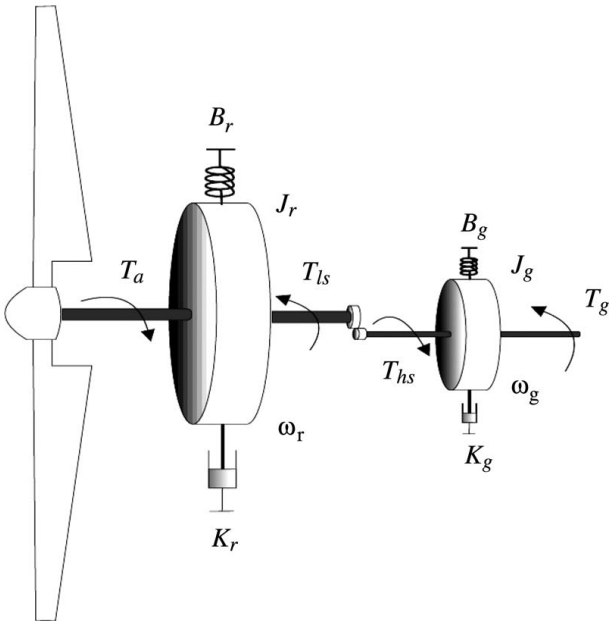

FIGURE 1. Schematic block diagram for the structure of VSWT [8]

Because of the gearbox ratio, the following relationship (3) is obtained for the speed ω_r, ω_g, and torque T_{ls}, T_{hs}.

$$n_g = \frac{\omega_g}{\omega_r} = \frac{T_{ls}}{T_{hs}} \tag{3}$$

According to the (1) to (3), and since $J_t \neq 0$, hence we can obtain

$$\dot{\omega}_r = \frac{1}{J_t}\left(T_a - K_t\omega_r - B_t\int_0^t \omega_r(\tau)\mathrm{d}\tau - T_g\right) \tag{4}$$

where $J_t = J_r + n_g^2 J_g$, $K_t = K_r + n_g^2 K_g$, $B_t = B_r + n_g^2 B_g$, $T_g = n_g T_{em}$. T_a and T_{em} can be described as follows [6,9],

$$T_a = K_w \cdot \omega_r^2,\ T_{em} = K_\phi \cdot c(I_f) \tag{5}$$

where K_w is a wind speed to power transfer parameter depending on factors like air density, radius of the rotor, the wind speed and the pitch angle. $c(I_f)$ is the flux in the generating system function. The electrical subsystem dynamics of VSWT is governed by [9]

$$\dot{I}_f = -\frac{R_f}{L}I_f + \frac{1}{L}u_f \tag{6}$$

Hence, from (4) to (6), the dynamic model of VSWT can be described as

$$\begin{cases} \dot{\omega}_r = \underbrace{\dfrac{K_w}{J_t}\omega_r^2 - \dfrac{K_t}{J_t}\omega_r - \dfrac{B_t}{J_t}\displaystyle\int_0^t \omega_r(\tau)\mathrm{d}\tau - \dfrac{n_g K_\phi}{J_t}c(I_f)}_{f_1(\omega_r,\theta_r,I_f)} \\ \dot{I}_f = -\dfrac{R_f}{L}I_f + \dfrac{1}{L}u_f \end{cases} \tag{7}$$

where angle $\theta_r = \int_0^t \omega_r(\tau)\mathrm{d}\tau$. Assume that function $f_1(\omega_r, \theta_r, I_f)$, R_f and L are all unknown. In practice, because of limit of the power and physical structure, the control input field voltage u_f cannot change too fast within a small time interval, and u_f magnitude cannot reach infinity. Hence, the control input u_f is subject to magnitude and rate constraints as follows:

$$u_f^{\min} \leq u_f \leq u_f^{\max} \quad \dot{u}_f^{\min} \leq \dot{u}_f \leq \dot{u}_f^{\max} \tag{8}$$

The control objective of this paper is to ensure that output rotor speed ω_r can follow a reference trajectory ω_d with field voltage u_f in the function $f_1(\omega_r, \theta_r, I_f)$, R_f and L being unknown. The controller design and the stability analysis also require the desired reference trajectory to be the first order integrable, that is

$$\int_0^T |\omega_d(\tau)| \, \mathrm{d}\tau < \infty$$

with T being finite (i.e., $\omega_d \in \mathcal{L}_1 \cap \mathcal{L}_\infty$ and $\dot{\omega}_d, \ddot{\omega}_d \in \mathcal{L}_\infty$).

3. **Main Results.**

3.1. **Model transformation.** Define new state $x_1 = \omega_r$, $x_2 = \dot{x}_1 = \dot{\omega}_r = f_1(\omega_r, \theta_r, I_f)$. Then the time derivative of x_2 can be expressed as

$$\begin{aligned} \dot{x}_2 &= \dot{f}_1(\omega_r, \theta_r, I_f) \\ &= \frac{\partial f_1(\omega_r, \theta_r, I_f)}{\partial \omega_r}\dot{\omega}_r + \frac{\partial f_1(\omega_r, \theta_r, I_f)}{\partial \theta_r}\omega_r + \frac{\partial f_1(\omega_r, \theta_r, I_f)}{\partial I_f}\dot{I}_f \\ &= f(\bar{x}) + g(\bar{x})u_f \end{aligned} \tag{9}$$

where

$$\begin{aligned} f(\bar{x}) &= f(\omega_r, \theta_r, I_f) \\ &= \frac{\partial f_1(\omega_r, \theta_r, I_f)}{\partial \omega_r} f_1(\omega_r, \theta_r, I_f) + \frac{\partial f_1(\omega_r, \theta_r, I_f)}{\partial \theta_r}\omega_r - \frac{R_f \cdot \partial f_1(\omega_r, \theta_r, I_f)}{L \cdot \partial I_f} \end{aligned}$$

and

$$g(\bar{x}) = g(\omega_r, \theta_r, I_f) = \frac{\partial f_1(\omega_r, \theta_r, I_f)}{L \cdot \partial I_f}$$

with $\bar{x} = [\omega_r, \theta_r, I_f]^T$. Hence, the dynamic model of VSWT (7) is now transformed as

$$\begin{cases} \dot{x}_1 = x_2 \\ \dot{x}_2 = f(\bar{x}) + g(\bar{x})u_f \\ \ \ y = x_1 \end{cases} \tag{10}$$

To account for the uncertainties in VSWT parameters, we rewrite the dynamics (10) as

$$\begin{cases} \dot{x}_1 = x_2 \\ \dot{x}_2 = d(t) + g_o u_f \\ \ \ y = x_1 \end{cases} \tag{11}$$

where g_o is the best available estimates of $g(\bar{x})$, while Δg is its associated uncertainties. The quantity $d(t) = f(\bar{x}) + \Delta g u_f$ is the combined uncertainty and may also include other sources such as external disturbance acting on the system.

3.2. **Extended state observer design.** We assume that only power angle $\omega_r = y$ can be measured for VSWT (7). So in this paper, the third-order ESO is designed, which is used to estimate the state x_2 and combined uncertainty $d(t)$. Define the combined uncertainty $d(t)$ as an extended state x_3. Let $x_3 = d(t)$, $\dot{x}_3 = \varpi$, where ϖ is an unknown function. We assume that $|\varpi(t)| < r$. Then system (11) is equivalent to

$$\begin{cases} \dot{x}_1 = x_2 \\ \dot{x}_2 = x_3 + g_o u_f \\ \dot{x}_3 = \varpi \\ \ \ y = x_1 \end{cases} \tag{12}$$

In order to estimate the state x_2 and combined uncertainty $d(t)$, we design the following third-order ESO [12,14]:

$$\begin{cases} \dot{\hat{x}}_1 = \hat{x}_2 - l_1\tilde{y} \\ \dot{\hat{x}}_2 = \hat{x}_3 + g_o u_f - l_2 \text{fal}(\tilde{y}, \alpha_1, \sigma_1) \\ \dot{\hat{x}}_3 = -l_3 \text{fal}(\tilde{y}, \alpha_2, \sigma_2) \\ \hat{y} = \hat{x}_1 \end{cases} \tag{13}$$

where $\tilde{y} = y - \hat{y} = x_1 - \hat{x}_1$ and $\hat{x}_1$, $\hat{x}_2$, $\hat{x}_3$ are the observer of x_1, x_2, x_3. $0 < \alpha_1 < 1$, $0 < \alpha_2 < 1$, $\sigma_1 > 0$, $\sigma_2 > 0$, $l_i > 0$, $i = 1, 2, 3$ are parameters of observer (13). And the nonlinear function fal$(\cdot)$ is defined as

$$\text{fal}(\epsilon, \alpha, \sigma) = \begin{cases} |\epsilon|^{\alpha}\text{sgn}(\epsilon), & |\epsilon| > \sigma \\ \dfrac{\epsilon}{\sigma^{1-\alpha}}, & |\epsilon| \le \sigma \end{cases} \tag{14}$$

Let T be sampling period of control, in generally, σ is selected as $\sigma = 5 \sim 10T$. Until now, there is no reliable theoretical analysis method available for the hird-order ESO. Fortunately, according to [12], if suitable parameters of observer (13) are selected, the following results can be obtained.

$$\lim_{t\to\infty} |\tilde{x}_2| < l_1 \left(\frac{r}{l_3}\right)^{1/\alpha_2} = \varepsilon_{x_2}, \quad \lim_{t\to\infty} |\tilde{d}| = \lim_{t\to\infty} |\tilde{x}_3| < l_2 \left(\frac{r}{l_3}\right)^{1/\alpha_2} = \varepsilon_d \tag{15}$$

where $\tilde{x}_2 = x_2 - \hat{x}_2$, $\tilde{d} = d - \hat{d}$, $\tilde{x}_3 = x_3 - \hat{x}_3$. Hence, we know the suitable observer parameters can make the state estimation errors $\tilde{x}_1$, $\tilde{x}_2$ and combined uncertainty error $\tilde{d} = \tilde{x}_3$ are uniformly ultimately bounded (UUB).

3.3. **Output feedback constrained controller design and stability analysis.** Define $x^d = \left[x_1^d, x_2^d\right]^T = \left[y^d, \dot{y}^d\right]^T$ with $y^d = \omega_d$. The ESO-based output feedback controller without input constraint can be designed as the following

$$u_f^* = \frac{1}{g_o}\left(-\hat{d}(t) + \ddot{y}^d + K^T e\right) \tag{16}$$

where $e = [e_1, e_2]^T = \left[y^d, \dot{y}^d\right]^T - [x_1, \hat{x}_2]^T$, and $K = [k_1, k_2]^T$ is the feedback gain vector determined such that $s^2 + k_2 s^1 + k_1$ is strictly Hurwitz.

Consider the input constraint (8), and then the controller (16) is evolved as

$$\begin{cases} u_{fc} = \dfrac{1}{g_o}\left(-\hat{d}(t) + \ddot{y}^d + K^T e + l_2 \text{fal}(\tilde{y}, \alpha_1, \sigma_1) + \zeta\right) \\ u_f = \text{Cons}(u_{fc}) \end{cases} \tag{17}$$

where ζ will be designed later. The block diagram of constraint function Cons(u_{fc}) can be described as Figure 2 [20,21]. Also its state-space dynamic model is given as

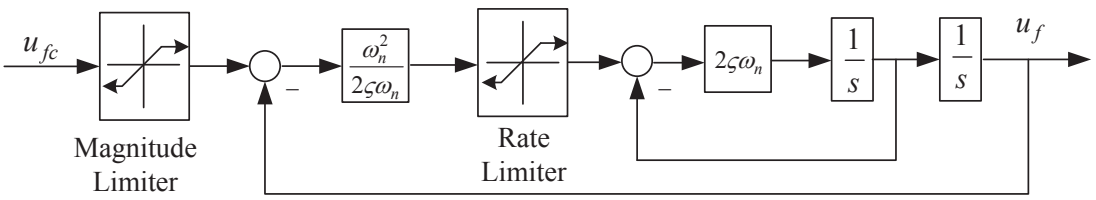

FIGURE 2. Structure of Cons(u_{fc})

$$\begin{cases} \dot{z}_1 = z_2 \\ \dot{z}_2 = 2\varsigma\omega_n \left[\mathrm{Sat}_r \left(\dfrac{\omega_n^2}{2\varsigma\omega_n} \left(\mathrm{Sat}_m(u_{fc}) - z_1 \right) \right) - z_2 \right] \\ u_f = z_1 \end{cases} \tag{18}$$

where ς and ω_n are the damping and the bandwidth of the filter, respectively. With $\mathrm{Sat}_r(\cdot)$ and $\mathrm{Sat}_m(\cdot)$ functions being defined as

$$\mathrm{Sat}_r(a) = \begin{cases} \dot{u}_f^{\max} & a \geq \dot{u}_f^{\max} \\ a & \dot{u}_f^{\min} < a < \dot{u}_f^{\max}, \\ \dot{u}_f^{\min} & a \leq \dot{u}_f^{\min} \end{cases} \quad \mathrm{Sat}_m(a) = \begin{cases} u_f^{\max} & a \geq u_f^{\max} \\ a & u_f^{\min} < a < u_f^{\max} \\ u_f^{\min} & a \leq u_f^{\min} \end{cases}$$

Redefine output tracking error $\bar{e} = [\bar{e}_1, \bar{e}_2]^T$ as

$$\bar{e}_1 = e_1 - \xi_1, \quad \bar{e}_2 = e_2 - \xi_2 \tag{19}$$

where

$$\begin{cases} \dot{\xi}_1 = \xi_2 \\ \dot{\xi}_2 = -\kappa_1\xi_1 - \kappa_2\xi_2 + g_o(u_{fc} - u_f) \end{cases} \tag{20}$$

(20) can be called "anti-windup compensator". Let $\xi = [\xi_1, \xi_2]^T$, and (20) can also be rewritten as

$$\dot{\xi} = A_1\xi + B_1\nu_1 \tag{21}$$

where $\nu_1 = g_o(u_{fc} - u_f)$ and

$$A_1 = \begin{bmatrix} 0 & 1 \\ -\kappa_1 & -\kappa_2 \end{bmatrix}, \; B_1 = \begin{bmatrix} 0 \\ 1 \end{bmatrix}$$

A_1 is the stability matrix, that is $s^2 + \kappa_2 s^1 + \kappa_1$ is strictly Hurwitz. If we design $\zeta = -k_1\xi_1 - k_2\xi_2$, from (19), (20) and control law (17), we have

$$\dot{\bar{e}} = A_2\bar{e} + B_2\nu_2 \tag{22}$$

where $\nu_2 = [\xi_1, \xi_2]^T$, and

$$A_2 = \begin{bmatrix} 0 & 1 \\ -k_1 & -k_2 \end{bmatrix}, \; B_2 = \begin{bmatrix} 0 & 0 \\ \kappa_1 & \kappa_2 \end{bmatrix}$$

The solution to (21) and (22) are

$$\xi(t) = \mathrm{e}^{A_1 t}\xi(0) + \int_0^t \mathrm{e}^{A_1(t-\tau)}B_1\nu_1(\tau)\mathrm{d}\tau, \quad \bar{e}(t) = \mathrm{e}^{A_2 t}\bar{e}(0) + \int_0^t \mathrm{e}^{A_2(t-\tau)}B_2\nu_2(\tau)\mathrm{d}\tau \tag{23}$$

Define $\bar{\nu}_1 = \sup_t |\nu|_1 = \Psi_1$, $\bar{\nu}_2 = \sup_t |\nu|_2 = \Psi_2$. And making the absolute value on both sides of (23) yields

$$\begin{aligned} |\xi(t)| &\leq \left|\mathrm{e}^{A_1 t}\right| |\xi(0)| + \int_0^t \left|\mathrm{e}^{A_1(t-\tau)}\right| \mathrm{d}\tau B_1\bar{\nu}_1 \leq m_1\mathrm{e}^{-\alpha_1 t}| \, |\xi(0)| + \frac{m_1 |B_1|}{\alpha_1}\Psi_1 \\ |\bar{e}(t)| &\leq \left|\mathrm{e}^{A_2 t}\right| |\bar{e}(0)| + \int_0^t \left|\mathrm{e}^{A_2(t-\tau)}\right| \mathrm{d}\tau B_2\bar{\nu}_2 \leq m_2\mathrm{e}^{-\alpha_2 t}| \, |\bar{e}(0)| + \frac{m_2 |B_2|}{\alpha_2}\Psi_2 \end{aligned} \tag{24}$$

where m_i and α_i are the positive constants that satisfy $\left|\mathrm{e}^{A_i(t-\tau)}\right| \leq m_i\mathrm{e}^{-\alpha_i(t-\tau)}$ with $i = 1, 2$. They can be made arbitrarily small by choosing sufficiently large $\alpha_2 \gg \alpha_1$. Hence, it can be seen that ξ and the redefined output tracking error $\bar{e}$ are UUB.

To give a clear idea of the overall design procedure, we give a flow chart as Figure 3.

Remark 3.1. *The observer law (13) and control law (17) are designed only by online measurable signal of VSWT. Compared with other control methods [5,6], [7-9], [10], explicit model dynamics and structural information of the VSWT do not need to be known for controller design.*

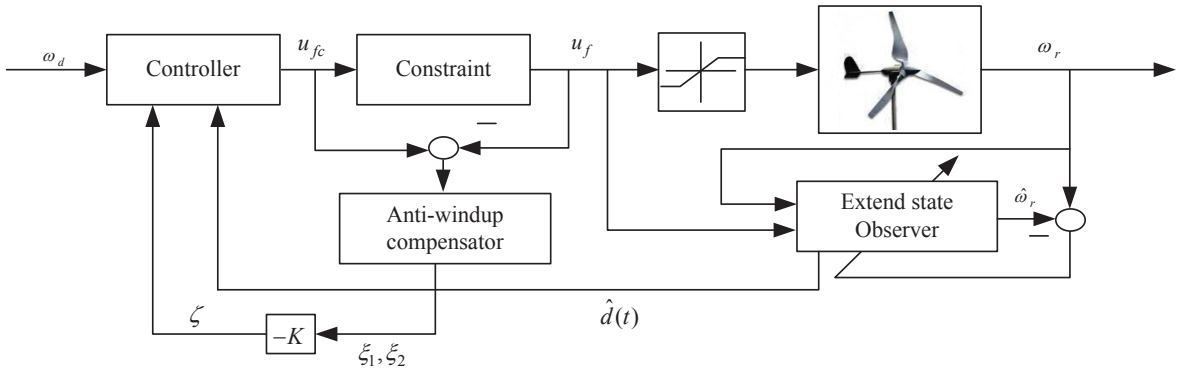

FIGURE 3. Proposed control scheme for VSWT

Remark 3.2. *Actuator magnitude and rate limitations are existing in VSWT because of physical constraint of electrical subsystem. We know, design the control law that ignore input constraints may cause the closed-loop system performance to degenerate or even unstablility. In this study, anti-windup compensator approach is used to accommodate the reference trajectory ω_d, which can ensure the control input within constraint range.*

4. **Simulation Results.** In this section, the simulation results are shown to demonstrate the validity of the proposed constrained control algorithm. In simulation, the system parameters of VSWT are chosen as the same as [6,9], which are considered as $R_f = 0.02\Omega$, $L = 0.001H$, $J_t = 24490$, $B_t = 52$, $K_t = 52$, $K_\omega = 3$, $n_g = 30$, $K_\phi = 1.7$, $c(I_f) = 1000I_f$.

And the reference angular velocity signal $\omega_d(t) = y^d$ is selected as:

$$\omega_d(t) = 2 + \sin(0.5t)$$

The cut-in wind speed $u_c = 4.3$m/sec, rated wind speed $u_r = 7.7$m/sec, furling wind speed $u_t = 17.9$m/sec. The constraints of control input u_f are given as

$$-0.008 \leq u_f \leq 0.008 \quad -0.005 \leq \dot{u}_f \leq 0.005$$

For the simulation, we choose ESO parameters as $l_1 = 10^2$, $l_2 = 10^4$, $l_3 = 10^5$, $\alpha_1 = \alpha_2 = 0.9$, $\sigma_1 = 10^2$, and $\sigma_2 = 10^3$. The parameters of anti-windup compensator are selected $\kappa_1 = 500$, $\kappa_2 = 500$. The controller gains are selected as $g_0 = -2000$, and $K = [5000, 5000]^T$. The initial state values are $\omega_r(0) = 1$, and $I_f(0) = 0$.

The results of simulation 1 (with sinusoidal reference trajectory) are shown in Figures 4-6, where Figure 4 illustrates the reference ω_d, actual rotor velocities ω_r , the field voltage u_f (control input), and rate of voltage u_f change ($\dot{u}_f$). Figure 5 shows the estimation errors for x_1, x_2 and $d(t)$. Figure 6 presents the responses of anti-windup compensator (20). It can be seen from the response figures, tracking and estimation errors converge to very small values, and furthermore the ESO-based output feedback constrained controller achieves good performance.

In addition, we have compared the proposed constrained control method with PID control and active disturbance rejection control (ADRC) [17]. In PID and ADRC simulation results, due to the facts that constraints of control input u_f are considered in VSWT's rotor speed control system, it makes rotor speed output capacity reduction and the field voltage cannot follow the supplied voltage.

5. **Conclusion.** In this paper, we have developed a nonlinear output feedback constrained control strategy based on ESO, which provides an alternative to the VSWT control problem. A dynamic constraints unit with anti-windup compensator scheme is adopted to keep control input within a safe range as long as possible. This proposed control approach of VSWT is particularly effective while the explicit analytical model of

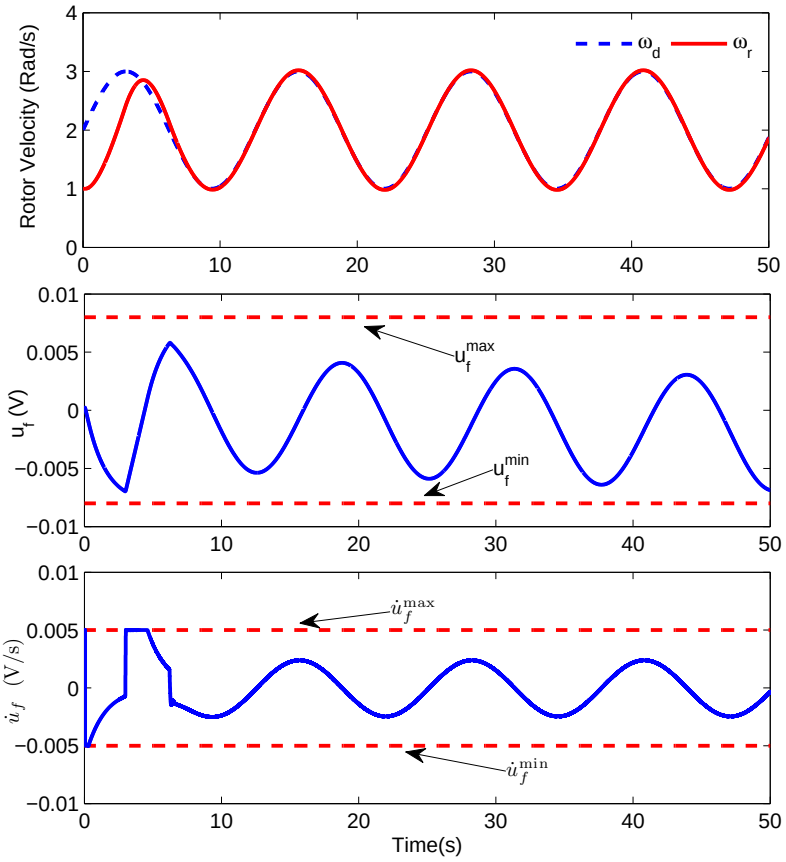

FIGURE 4. The VSWT output and control input responses curve

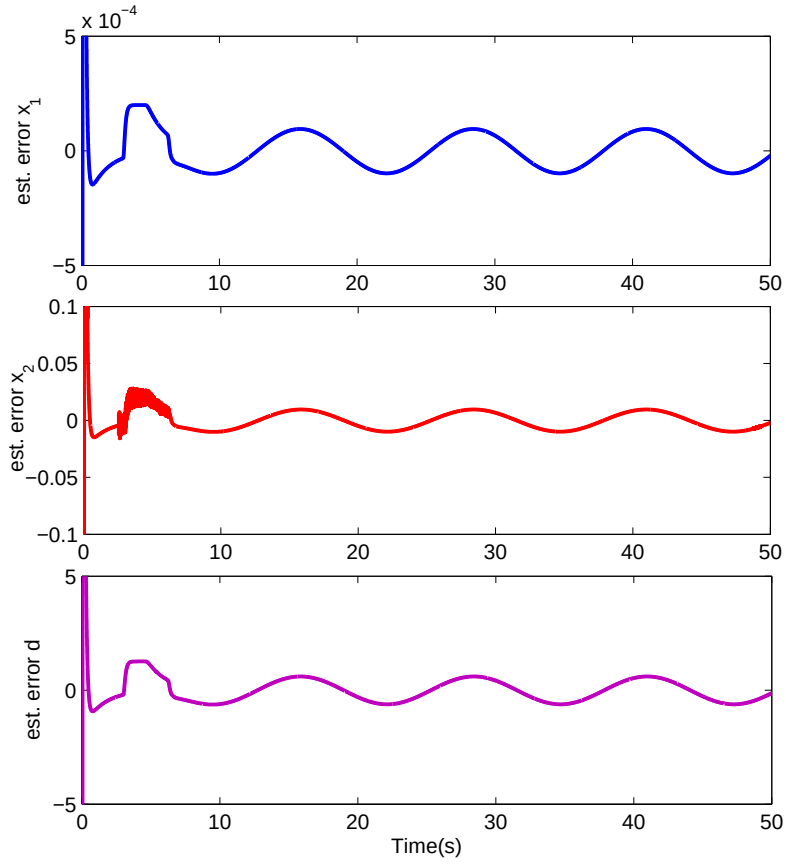

FIGURE 5. The state estimation errors by ESO

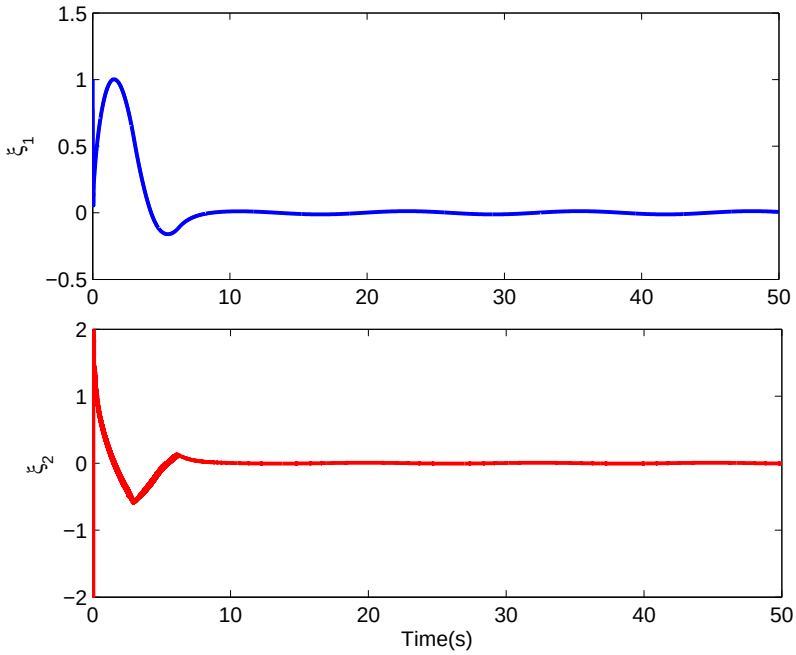

FIGURE 6. The responses of anti-windup compensator

VSWT is difficult to be described and the states are not fully measurable. Our focus of this paper is on the uncertainty, states incomplete measurable and control input saturation. The simulation results have validated the proposed nonlinear constrained control algorithm. Fault-tolerant control is our future research direction.

Acknowledgment. This work is supported by the National Natural Science Foundation of China (61503156, 51405198) and the Fundamental Research Funds for the Central Universities (JUSRP11562, JUSRP51406A, NJ20150011) and National Key Research and Development Program (2016YFD0400300) and the Science and Technology Funds for Jiangsu China (BY2015019-24).

REFERENCES

[1] X. Zhao, Z. Yan and X.-P. Zhang, A wind-wave farm system with self-energy storage and smoothed power output, *IEEE Access*, vol.4, pp.8634-8642, 2016.

[2] Z. Chen, J. M. Guerrero and F. Blaabjerg, A review of the state of the art of power electronics for wind turbines, *IEEE Trans. Power Electronics*, vol.24, no.8, pp.1859-1875, 2009.

[3] P. Xiong, P. Jirutitijaroen and C. Singh, A distributionally robust optimization model for unit commitment considering uncertain wind power generation, *IEEE Trans. Power Systems*, vol.32, no.1, pp.39-49, 2017.

[4] T. Burton, D. Sharpe, N. Jenkins and E. Bossanyi, *Wind Energy Handbook*, Wiley, Hoboken, NJ, 2001.

[5] O. Barambones, J. M. Durana and M. D. Sen, Robust speed control for a variable speed wind turbine, *International Journal of Innovative Computing, Information and Control*, vol.8, no.11, pp.7627-7640, 2012.

[6] K. Yenduri and P. Sensarma, Maximum power point tracking of variable speed wind turbines with flexible shaft, *IEEE Trans. Sustainable Energy*, vol.7, no.3, pp.956-965, 2016.

[7] B. Boukhezzar and H. Siguerdidjane, Nonlinear control of a variable speed wind turbine using a two-mass model, *IEEE Trans. Energy Conversion*, vol.26, no.1, pp.149-162, 2011.

[8] Y. Bao, H. Wang and J. Zhang, Adaptive inverse control of variable speed wind turbine, *Nonlinear Dynamics*, vol.61, no.4, pp.819-827, 2010.

[9] C. Caruana, A. Al-Durra and F. Blaabjerg, Observer-based scheme for tuning the control of variable speed wind turbines operating in hostile environments, *IET Renewable Power Generation*, vol.10, no.3, pp.418-425, 2016.

[10] B. Beltran, T. Ahmed-Ali, M. E. Benbouzid, High order sliding-mode control of variable-speed wind turbines, *IEEE Trans. Industrial Electronics*, vol.56, no.9, pp.3314-3321, 2009.
[11] W. Meng, Q. Yang and Y. Sun, Guaranteed performance control of DFIG variable-speed wind turbines, *IEEE Trans. Control Systems Technology*, vol.24, no.6, pp.2215-2223, 2016.
[12] F. Wu and M. Soto, Extended LTI anti-windup control with actuator magnitude and rate saturations, *Proc. of the 42nd IEEE Conference on Decision and Control*, pp.2784-2789, 2003.
[13] M. Ran, Q. Wang, C. Dong and M. Ni, Simultaneous anti-windup synthesis for linear systems subject to actuator saturation, *Journal of Systems Engineering and Electronics*, vol.26, no.1, pp.119-126, 2015.
[14] A. Bateman and Z. Lin, An analysis and design method for linear systems under nested saturation, *Systems and Control Letters*, vol.48, no.1, pp.41-52, 2003.
[15] M. Fiacchini, S. Tarbouriech and C. Prieur, Quadratic stability for hybrid systems with nested saturations, *IEEE Trans. Automatic Control*, vol.57, no.7, pp.1832-1838, 2012.
[16] T. M. Chan, K. F. Man et al., A jumping gene paradigm for evolutionary multiobjective optimization, *IEEE Trans. Evolutionary Computation*, vol.12, no.2, pp.143-159, 2008.
[17] J. Han, From PID to active disturbance rejection control, *IEEE Trans. Industrial Electronics*, vol.56, no.3, pp.900-906, 2009.
[18] C. Liu, G. Liu and J. Fang, Feedback linearization and extended state observer-based control for rotor – AMBs system with mismatched uncertainties, *IEEE Trans. Industrial Electronics*, vol.64, no.2, pp.1313-1322, 2017.
[19] Y. Huang, K. Xu, J. Han and J. Lam, Flight control design using extended state observer and non-smooth feedback, *Proc. of the 40th IEEE Conference on Decision and Control*, Orlando, FL, pp.223-228, 2001.
[20] B. Jiang, D. Xu, P. Shi and C. Lim, Adaptive neural observer-based backstepping fault tolerant control for near space vehicle under control effector damage, *IET Control Theory and Applications*, vol.8, no.9, pp.658-666, 2014.
[21] D. Xu, B. Jiang, H. Liu and P. Shi, Decentralized asymptotic fault tolerant control of near space vehicle with high order actuator dynamics, *Journal of the Franklin Institute*, vol.350, pp.2519-2534, 2013.